

Article

Cold Hardiness of *Prunus mume* ‘Xiang Ruibai’ and Its Parents Based on Biological Indexes and Physical Parameters

Anqi Ding^{1,2,3,4}, Fei Bao^{2,3,4} , Aiqin Ding^{2,3,4} and Qixiang Zhang^{2,3,4,*}

- ¹ College of Tourism and Urban-Rural Planning, Chengdu University of Technology, Chengdu 610059, China
² Beijing Key Laboratory of Ornamental Plants Germplasm Innovation & Molecular Breeding, Beijing Forestry University, Beijing 100083, China
³ National Engineering Research Center for Floriculture, Beijing Forestry University, Beijing 100083, China
⁴ School of Landscape Architecture, Beijing Forestry University, Beijing 100083, China
* Correspondence: zqxbjfu@126.com; Tel.: +86-1062338005; Fax: +86-1062336321

Abstract: Low temperature is a primary factor limiting the distribution of *Prunus mume*. In order to produce a variety that has both cold tolerance and the characteristic fragrance of true *mume*, previous researchers crossbred a strong-tolerance variety apricot mei, *P. mume* ‘DF’ (‘Dan Fenghou’) and the weak-tolerance variety of true *mume*, *P. mume* ‘BY’ (‘Beijing Yudie’). They gained an offspring variety named *P. mume* ‘XR’ (‘Xiang Ruibai’), but its cold tolerance is unknown at this point. Here, three varieties (XR, BY, and DF) were selected as the materials, and different low-temperature treatments were used, with temperature as the only variable. Conventional biological methods, such as ion leakage rate, different tissues, and plant viability statistics, were used, as well as an innovative use of infrared engineering and moisture monitoring for dynamic observation of the water-to-ice process in tissues. The results were as follows: DF cold tolerance was the highest, followed by XR and then BY. The LT₅₀ of XR was increased by 6 °C after five days of cold priming at 4 °C, which indicated a stronger cold acclimation ability than the parent varieties. The XR variety enhanced the antioxidant capacity by increasing SOD and POD enzyme activities during low temperature treatment, thus enhancing the cold tolerance. The antioxidant enzyme genes *PmSOD3*, *PmPOD2*, *PmPOD19*, and *PmPOD22* had important regulatory roles in XR’s cold acclimation process.

Keywords: cold tolerance; *Prunus mume* ‘Xiang Ruibai’; infrared detection; LT₅₀; antioxidant capacity



Citation: Ding, A.; Bao, F.; Ding, A.; Zhang, Q. Cold Hardiness of *Prunus mume* ‘Xiang Ruibai’ and Its Parents Based on Biological Indexes and Physical Parameters. *Forests* **2022**, *13*, 2163. <https://doi.org/10.3390/f13122163>

Academic Editor: Stefan Arndt

Received: 11 September 2022

Accepted: 13 December 2022

Published: 16 December 2022

Publisher’s Note: MDPI stays neutral with regard to jurisdictional claims in published maps and institutional affiliations.



Copyright: © 2022 by the authors. Licensee MDPI, Basel, Switzerland. This article is an open access article distributed under the terms and conditions of the Creative Commons Attribution (CC BY) license (<https://creativecommons.org/licenses/by/4.0/>).

1. Introduction

Prunus mume Sieb. et Zucc. (mei) from the Rosaceae family is a species widely used as a traditional ornamental flowering plant and fruit tree in China. Mei flowers bring vitality and contribute to the diversity of flower varieties in early spring. However, they grow along the Yangtze River basin and cannot overwinter outdoors in the north of China. To expand distribution, the breeding of cold-resistant varieties has been conducted for nearly half a century. Since the 1950s, Chen and Zhang have cultivated a population of cold-tolerant mei varieties through introduction and hybridization, including FH (‘Feng Hou’), DF (‘Dan Fenghou’), YX (‘Yan Xing’), and BM (‘*Blireiana* Mei’) [1–4]. According to the source of the hybrids, the offspring of apricot and mei plants are divided into the apricot mei group, while the offspring of plum and mei plants are divided into the *Blireiana* group. Native mei varieties are called true *mume* [5]. In regional survival tests on the cold tolerance of mei varieties, three major groups have been classified: apricot mei > *blireiana* > true *mume* [4,6–8]. In studies on cold tolerance, the apricot mei group is represented by YX, FH, DF, and ‘SC’ (‘Song Chun’), which was able to withstand the low temperature of −30 °C in regional survival tests. The true *mume* ‘BY’ (‘Beijing Yudie’) had moderate cold tolerance and required a certain microclimate to be cultivated in an open field in Beijing [4,7,9]. Although apricot mei varieties inherit the strong cold tolerance of apricots, they lose the characteristic floral aroma of true *mume*, except for the ‘XR’ variety (‘Xiang Ruibai’). The

'XR' variety studied in our research is a hybrid obtained by Chen in 1999, with the apricot mei DF as the female parent and the true *mume* BY the male one. It emits the characteristic floral aroma of true *mume* and has great research and development potential [10]. However, an evaluation of its cold tolerance has never been reported.

With temperature as a parameter, injuries caused at 0 °C or above are termed 'chilling damage', while those below 0 °C are called 'frost damage'. Chilling damage can cause plant photosynthesis, cell membrane fluidity, and a decrease in basal metabolism, and therefore, plant growth and development are inhibited. Frost damage can lead to the direct mechanical damage, and even death, of plant cells [11–13]. Tolerance to low temperature varies in different species. For example, the *japonica* variety of rice can tolerate low temperatures in boreal regions, but the *indica* variety cannot [14]. A complex and sophisticated mechanism of tolerance to low temperatures can be developed in plants through low-temperature acclimation and undercooling. Low-temperature acclimation refers to the process of treating plants at a low temperature that does not cause serious injury but instead leads to significantly higher freezing tolerance in plants [12,15–17]. It includes cold and freezing acclimation for woody plants and enhances cell membrane permeability, which can prevent the formation of intracellular ice crystals [18]. Undercooling refers to the phenomenon where water does not freeze when the temperature drops below freezing; it is an important way to avoid freezing injuries in plant tissue cells [19–22].

As early as the 1970s, Lyons and Raison demonstrated that, when plants are exposed to low temperatures, the stimulation of membrane lipids results in a series of changes that increase membrane permeability, which can lead to cell bursting and large amounts of dielectric exocytosis [23]. The increase in the cell membrane permeability of cold-tolerant varieties is minor and easily restored, while the cell membranes of varieties that have poor cold tolerance are easily damaged. Therefore, the change in electrolyte extravasation can be measured as a scale of cold tolerance in plants [24–27]. In addition, the logistic equation can be used to determine the semi-lethal temperature (LT₅₀) and the critical lethal temperature of plants [25,28,29]. Zhang evaluated and compared the cold tolerance of 38 *Prunus mume* varieties using conductivity and growth recovery [6,26]. Other studies have recognized conductance as a reliable parameter for determining the cold tolerance of cotton, grapevines, plums, hazelnuts, fig, apricots, and their interspecific hybrids [26,30–33].

The freeze–thaw ability of plants has an important effect on the survival and growth of plants and assists in evaluating their freezing tolerance and, thus, selecting strong-tolerance plants [34–36]. The plant freeze–thaw ability leads to temperature changes through exothermic or endothermic processes [24]. Detecting the formation and development of ice crystals in plants during the freeze–thaw process is of great significance. In early research, the internal structures of plant tissues have been observed and dissected in laboratory settings, and the biochemical indicators of plant tissues have been analyzed to determine their freeze–thaw situations [37–39]. Infrared spectroscopy, nuclear magnetic resonance imaging, and impedance spectroscopy have also been used for freeze–thaw detection [40–42]. Infrared thermal imaging was used to directly observe ice nuclei, where the ice initially formed and then expanded in plants [43]. *Prunus persica* and *Malus domestica* apples have inherent ice-nucleating agents that are highly active at low temperatures, and ice-nucleated bacteria may induce them to bloom or freeze [44,45]. Icing in plants was found to be sequential: it started from the bark outside the stem and then spread to primary tissues, such as flower buds and young branches [46]. Based on the dielectric and exotherm temperature principle, sensors have been investigated to analyze variations in water and ice content in stems [47–51].

In this study, the true *mume* BY, the apricot mei DF, and their progeny XR were treated with artificial gradient cooling to study their cold tolerance. The methods of morphology, section observation, tissue browning, ion leakage rate, infrared thermal-imaging technology, and freeze–thaw detection sensors were used. The results were applied together to analyze the cold tolerance of the three varieties and to provide a preliminary study on the mechanism of elevated cold acclimation ability in XR.

2. Materials and Methods

2.1. Plant Materials and Treatments

The three *P. mume* cultivars (apricot mei 'DF', true *mume* 'BY', and their hybrid offspring 'XR') were grown at two sites in Beijing, China: (i) Jiufeng National Forest Park (39°54' N, 116°28' E, 800 m.a.s.l.); and (ii) Beijing Forestry University (40°00' N, 116°34' E, 200 m.a.s.l.). Grafted seedlings were chosen to corroborate the results of adult trees and avoid errors caused by discrete branches (Supplementary Materials Figure S1).

The twigs of annual branches and stems of the three varieties adult trees were harvested before (September 2018 when the fallen leaf scars appear at the petiole) and after winter (February 2019 when flower buds and leaf buds start to sprout). They were treated at a steady rate of $-0.5/K\ h$ down to 4, 0, -5 , -10 , -15 , -20 , -25 , -30 and $-40\ ^\circ\text{C}$ in a temperature-alternating test chamber (Qieke, Beijing, China). The air temperature was then held at the target temperature for 1 h, and stems were thawed at a rate of 5 K/h and warmed to 4 °C. The twigs can be used to measure ion leakage, freezing tolerance, paraffin section and infrared video thermography. Adult tree branches of BY and DF in the field were measured for stem water content with a stem moisture sensor. The purpose of this was to observe the pattern of freezing and thawing of water in the branches of true *mume* BY and apricot mei DF grown in the one field environment in winter.

Grafted to *Armeniaca sibirica* (L.), Lam seedlings can be used as juvenile tree material to measure ion leakage, freezing tolerance, infrared video thermography, SOD and POD activity and gene expression. They were selected after 5 d of cold accumulation at 4 °C and cold accumulation ability was compared with the unaccumulation material. Accumulation and unaccumulation grafted seedlings were treated as whole plants in the cabinet refrigerator (SC/SD-332C, Haier, Shandong, China). The temperature inside the cabinet refrigerator was regulated by an external high-precision intelligent thermostat switch (LUEABB, SM6-LCD). Treating with a cooling rate of 1 °C /1 h to 4, 0, -5 , -10 , -15 , $-20\ ^\circ\text{C}$ and each gradient was maintained for 12 h, with the 25 °C material as the control. The material was then taken at each gradient temperature point and thawed at 4 °C for 12 h. The treated stems were used for ion leakage, freezing tolerance measuring and infrared video thermography observing. The other grafted seedlings of the three varieties experienced chilling treatment (4 °C for 8 h and 5 d), freezing treatment ($-5\ ^\circ\text{C}$ for 1 h) and recovery to 4 °C after freezing (1 °C /1 h). Then, the stems were used for SOD and POD activity measuring, transcriptome sequencing and gene expression analysis. More than three biological replicates were performed.

2.2. Measurement of Ion Leakage

The twigs of annual branches and grafted seedlings stems were rinsed with deionized water. Six 0.5 cm long branches without buds were cut and inserted into one glass test tube with 10 mL of deionized water, with three biological and technical replications. The tubes were incubated at 25 °C for 8h and the electrical conductivity of the water bath with the segments (S_{initial}) was measured (FG3-FK Conductivity Meter, Mettler Toledo, Zurich, Switzerland). To measure the maximal conductivity (S_{total}), the tubes were incubated in a water bath at 100 °C for 30 min and subsequently cooled at 25 °C for 30 min. The extent of ion leakage from tubes without branches (S_0) was determined. The index of cell membrane injury (L) was estimated according to Zhang et al. (1985):

$$L = 100 (S_{\text{initial}} - S_0) / (S_{\text{total}} - S_0) [\%]$$

The low semi-lethal temperature (LT_{50}) was calculated by fitting the logistic equation the with electrolyte exudation rate [52].

2.3. Determination of Freezing Tolerance

The cold tolerance of vegetative and reproductive shoots of adult trees and grafted seedlings was evaluated by placing the materials at a range of freezing temperatures. At

least four twigs bearing numerous reproductive and vegetative shoots were randomly selected from the sample pools of the three varieties. Twig samples were exposed in a hydroponic bottle at 4 °C for 12 h before initiating the freezing protocol. The freezing protocol was the same as that of ion leakage measurement. Then, hydroponic twigs were placed at day and night temperatures of 25 and 22 °C, respectively, with light of 1000 lx for 14 h per day for one week to allow frostbite to develop or recover. The injury to shoots was assessed with the degree of browning discoloration (n = 24 to 71 shoots per exposure temperature). Buds die if they are attacked by frost, so their statistics were either undamaged (0%) or frost-killed (100%). All the samples were observed under a stereomicroscope (Shanghai, China).

2.4. Paraffin Section

Stem samples of the three varieties of adult trees were divided into two treatment groups, which were, respectively, treated at 4 and −30 °C for 5 h, thawed, and stored in FAA solution (formaldehyde: glacial acetic acid: 70% ethanol = 1: 1: 18 *v/v*). The samples were dehydrated in a gradient ethanol series for 1 h (70%, 85%, 95%, and 100%) and embedded in paraffin. Sections at a thickness of 8 µm were fixed on silane-coated slides when the paraffin was melted but the tissue samples remained. Afterward, the samples were dehydrated using a gradient ethanol series and dyed with safranin o-fast green staining. Finally, the sections were observed with an automatic microscope (Panoramic MIDI, 3DHISTECH Ltd., Budapest, Hungary).

2.5. Infrared Video Thermography

The exothermic reaction during icing allowed us to observe the critical freezing temperatures of different tissues of the three varieties. Selected detached twigs of adult trees and intact grafted seedlings were used as material. The experiments were conducted in two types of controlled environment chambers: a horizontally adjustable temperature refrigerator (SC/SD-332c, Haier, Shandong, China) or an external microcomputer intelligent temperature controller (LB-SM6, Lueabb, Wenzhou, China). The temperature remained stable after placing thermometers at three different sites in the chambers. Temperature changes and ice in plants were monitored with an infrared thermal imager (Ti55FT, Fluke, State of Washington, USA). Infrared images were recorded with one photo every two seconds, and the fluctuation in temperature was also noted. Exothermal activity in the plants was monitored synchronously to generate a real-time heat map. As the water turned into ice, a large amount of latent heat from fusion was released, and the temperature rose. The greater the amount and range of frozen water, the longer and more obvious the reaction. The whole procedure was repeated at least nine times.

2.6. Measurement of Stem Water Content in Field by Stem Moisture Sensor

Based on the principle of standing wave rate [53], the arbor stem moisture sensor consisted of a signal source, a coaxial transmission line, and a two-pin parallel stainless-steel probe. Perennial branches with diameters of 10 cm on adult trees of DF and BY in field were selected. A hole was drilled at a distance of 1 m from the ground, and probes to measure voltage and temperature were placed. The dielectric properties of the arbor stem determined the degree of the voltage difference across the coaxial transmission line (i.e., the output voltage of the sensor). The collected data were remotely transmitted to a smart forestry ecological detection platform via GPRS (general packet radio service), which generated the visualized microenvironment. Using a standard curve, the output voltage value could be converted to the volume of water content in the trunk. It was drawn by collecting isolated stems of the same thickness from the chosen trees and by measuring the voltage value in the natural environment after fully absorbing water (Supplementary

Materials Figure S2). Combined with the temperature and water content values, the freezing volume of the moisture in the stem could be calculated with the following formula [51]:

$$V_{\text{ice}} = \pi(R^2 - r^2)H\theta_A^* \rho_w / \rho_{\text{ice}}$$

where V_{ice} is the freezing volume; R is the stem radius; r is the radius of stems that were not frozen or thawed during the freeze–thaw process; H is the stem length measured by sensor; θ_A is the θ_{Stem} volume of moisture content at the freezing point; ρ_w is the density of water; and ρ_{ice} is the density of ice.

2.7. SOD and POD Activity Determination

The stems of grafted seedlings that experienced chilling treatment (4 °C for 8 h and 5 d), freezing treatment (−5 °C for 1 h) and recovery to 4 °C after freezing (1 °C/1 h) were chosen. SOD and POD enzyme activities were determined using NBT and guaiacol methods [54]. Sample powder (0.05 g) was homogenized in 1.2 mL of 0.05 M phosphate buffer (PH 7.8) in an ice bath and centrifuged at 10,000× g for 15 min at 4 °C. The supernatant was replaced with SOD and POD enzyme solutions. NBT and guaiacol methods were used to measure SOD and POD activities [54]. The absorbances were measured at 560 nm and 240 nm, respectively, with an ultraviolet spectrophotometer. The SOD and POD activities were calculated according to the standard curve and dilution of the supernatant. Each treatment was performed in triplicate.

2.8. Gene Expression Analysis and Validation

The materials same as SOD and POD activity determination were used for transcriptome sequencing. Heat maps of SOD- and POD-enzyme-related genes in low-temperature stress were visualized with TBtools based on RPKM (reads per Kilobase of exon model per million mapped reads) values.

Total RNA of the stems for transcriptome sequencing was isolated with an RNA Extraction Kit (Tiangen, Beijing, China), and for reverse transcription into cDNA, we used a FastQuant RT Kit (TIANGEN, Beijing, China). cDNA (2 μ L) was used as the template in a 10 μ L qRT-PCR instrument with TB Green IIPremix Ex Taq (TaKaRa, Dalian, China). The relative expression levels were calculated using the $2^{-\Delta\Delta C_t}$ method, and the *Ubiquitin 2* (*UBQ2*) gene of *P. mume* was used as the internal control [55]. The four selected genes and specific primers are listed in Supplementary Table S1. Each qRT-PCR was repeated at least three times.

2.9. Statistical Analysis

Each group of experiments was repeated three times, and the average values were used to calculate the significance of each variety. The significance was tested with a single-factor analysis of variance (Duncan's multiple comparison analysis), where * indicates $p < 0.05$. A three-variable linear regression formula was applied for modeling. SPSS 26 (SPSS Inc., Chicago, IL, USA) was used for the whole analysis.

3. Results

3.1. Heat Release and Icing of Different Varieties of *P. mume* at Low Temperatures

The freezing rate of water in a plant is affected by various factors, such as environmental temperature, moisture content, osmotic potential, and ice cores. We found that water generated heat when turning to ice in the stems and buds, as shown in Figure 1A,B. During the freezing process, the tissue temperature increased by at least 2 °C. In the experimental process, we recorded the surface temperatures of the plants before exotherm as the freezing-point temperatures. The changes in the trends of freezing-point temperatures of the three varieties at different ages were the same. BY was the highest, while DF was the lowest (Figure 1C,E). The temperatures ranged from −3 to −6 °C (adult trees) and from −1 to −5 °C (grafted seedlings). During the observation process, it was found that the highest freezing rate of DF was caused by the intracellular moisture content

(Supplementary Materials Figure S3). We also studied the changes in ice patterns in flower buds and found that the freezing-point temperatures and freezing rates were lower than those of the branches (Supplementary Materials Figures S4 and S5). The freezing-point temperature of flower buds was in the range of -6 to -8 °C, and the change in the trend of the three varieties was contrary to the results for the branches: BY was the lowest and DF was the highest.

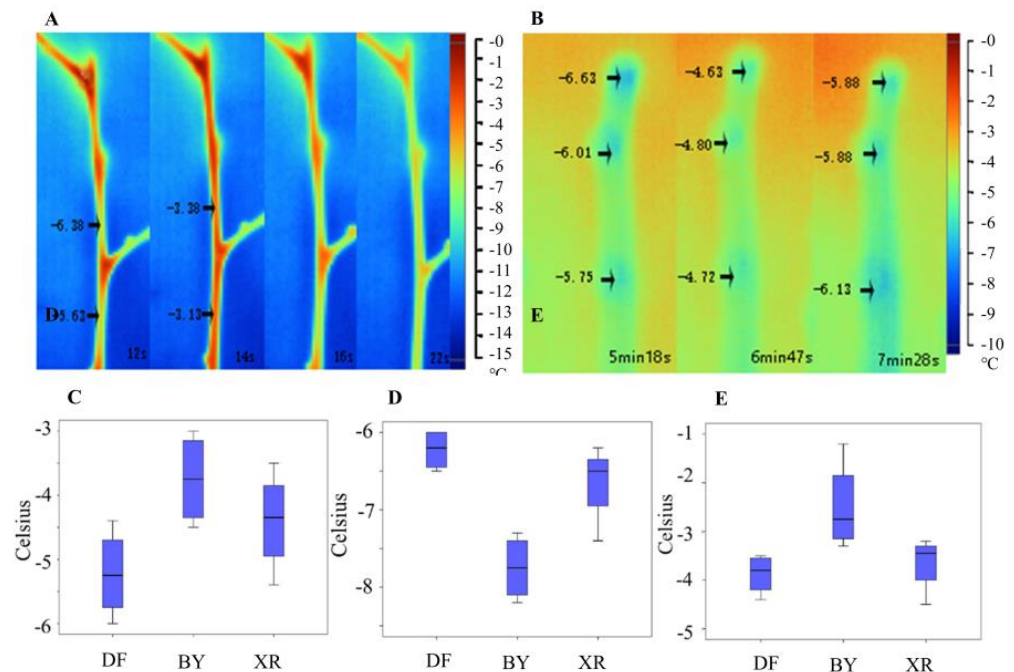


Figure 1. Branch and bud freezing temperature statistics and diagrams of the exothermic processes of icing. Diagrams of the icing processes of stems (A); and buds (B) in XR captured with infrared cameras. Box diagrams based on icing temperature statistics (C–E): (C), one-year-old branches of mature trees; (D), flower buds of mature trees; and (E), branches of one-year-old grafted seedlings.

We supplemented the observations of the moisture, temperature, and ice content changes with those of live *P. mume* trees in the field (Figure 2). The results showed that the stems of plants that were detected in winter underwent freeze–thaw changes every day. This repeated freeze–thaw phenomenon was likely to cause one-year-old branches to rupture and dehydrate, and this was observed from a process named the tipping phenomenon. The results showed that the DF freezing-point temperature was higher than that of BY most of the time, which was not consistent with the infrared results (Figure 1C–E). These results drew our attention to the fact that the water content of DF was consistently higher than that of BY, which could be due to the difference in basal water content between the two varieties. Despite the errors in the basal water content, two peaks in the graph (from 19 to 23 December and from 29 December to 4 January) revealed substantial icing results for BY (green frames in Figure 2). These results could still corroborate the infrared observation results.

3.2. Damage and Cold-Tolerance Ability of Different Varieties of *P. mume*

There were significant differences among the three varieties in the results of the ion leakage rate (Figure 3A, B). When the ambient temperature dropped to -30 °C, the ion leakage rate of DF was still below 50%, while BY was already above 50% at -20 °C and exceeded 70% at -30 °C. The LT_{50} also showed that the lethal temperature of DF was lower than those of XR and BY. The analysis of material from the adult trees using the isolated branches and planting environments of the three varieties was inconsistent, so this study also used the data of one-year-old grafted seedlings to corroborate the results of

the adult trees (Figure 3C). The results showed that the LT_{50} for the seedlings was lower than that of adult trees because the one-year-old seedlings were weaker, but the change in the trend of the three varieties was consistent. The cold acclimation abilities of the three varieties (18 November and 19 February) were compared. The degree of cell rupture under cold stress in the plants was reduced after deep winter, and the LT_{50} increased by 2–4 °C (Figure 3A,B). However, it was difficult to observe the effect of cold acclimation for the 20-year-old adult trees, so grafted seedlings that had not experienced low temperatures were selected. Figure 3D–F shows that the three varieties were placed in a 4 °C environment for five days to achieve cold acclimation that could withstand temperatures above –10 °C, and the results were much stronger than materials not pretreated at 4 °C. A comparison of the three varieties found that the cold acclimation ability of XR was stronger than both its parents, and the LT_{50} after cold acclimation increased by 6 °C.

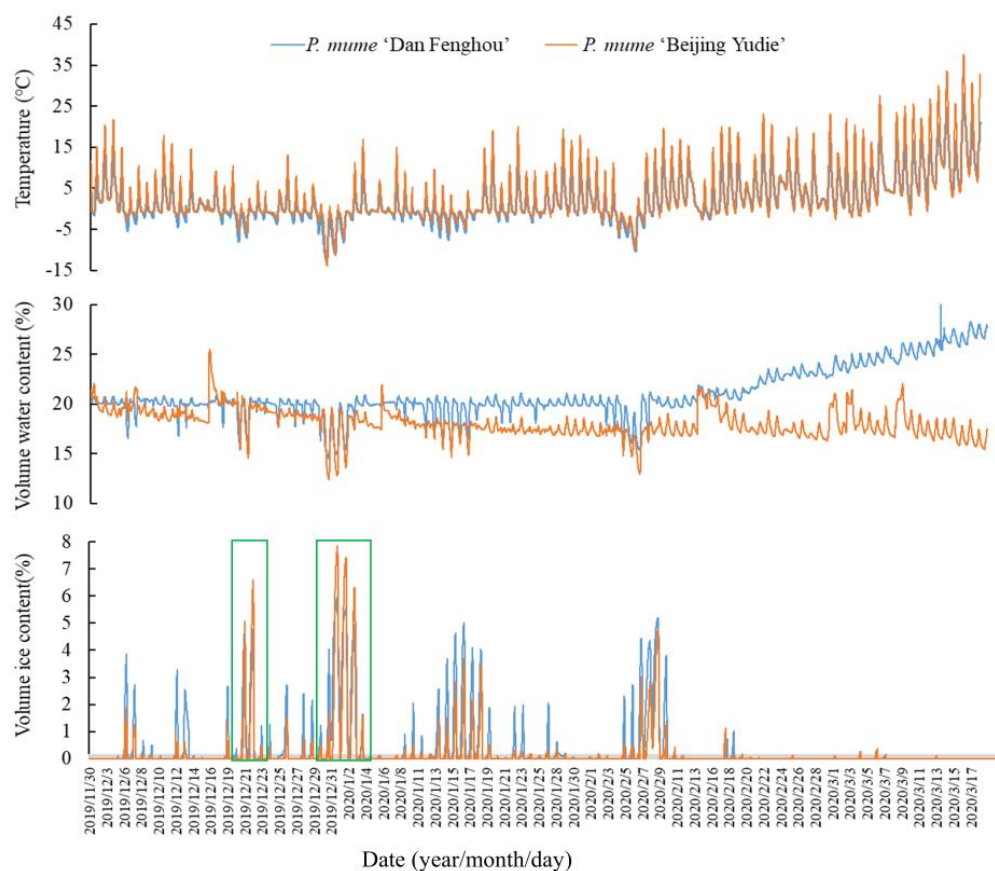


Figure 2. Dynamic monitoring of temperature, moisture content, and ice conditions during overwintering of adult trees of apricot mei DF and true *mume* BY.

We used the degree of stem restoration to evaluate the recovery abilities of the three varieties after low-temperature treatment (Figure 4A–G). When the temperature was below –20 °C, the branches of the three varieties turned brown and moldy after recovery. The interiors of the stems were also heavily waterlogged (Figure 4E–G). Paraffin sections provided a good view of the cellular changes within the stems. The ice crystal extrusion caused many voids in the tissues after freezing treatment. Due to different cold tolerance levels, the size of the ice voids in the three varieties was different. Because of the lower tissue density, the stems of BY had a large number of voids in the cortex and phloem fiber. The offspring, XR, had the same phenomenon as BY, but the void distribution and tissue rupture were relatively mild.

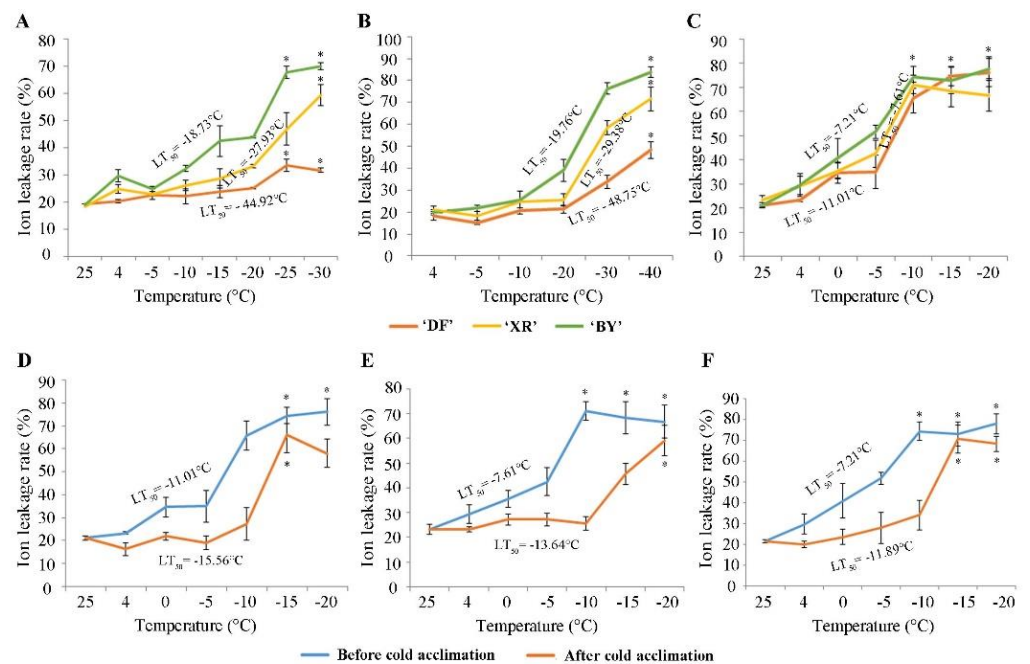


Figure 3. Changes in ion leakage rates and effects of cold acclimation of DF, XR, and BY. Adult trees before (A); and after (B) winter. Grafted seedlings of three varieties (C); and each variety before and after cold acclimation: (D) DF; (E) XR; and (F) BY. $p < 0.05$, marked by *.

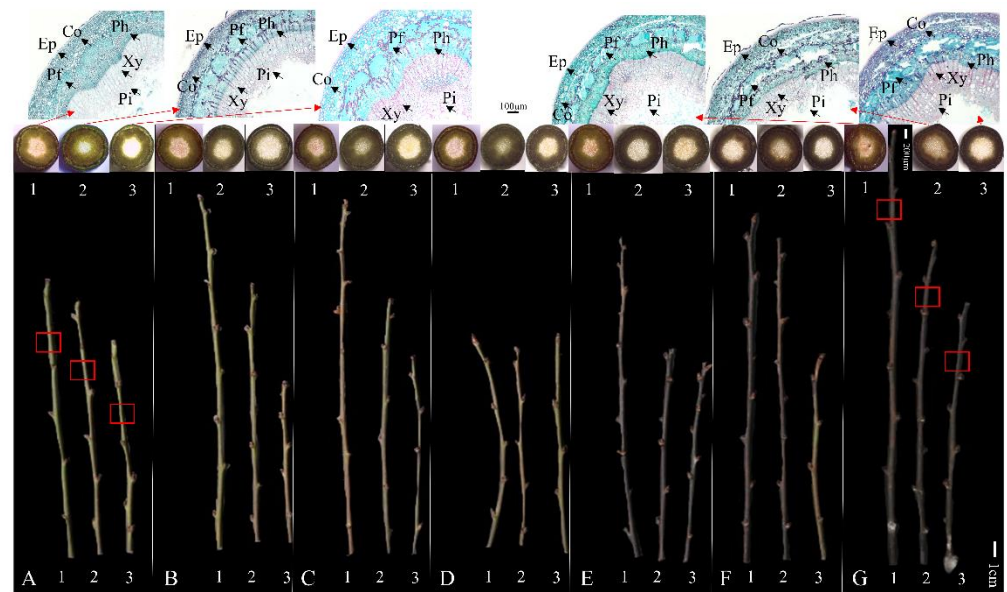


Figure 4. Freehand and paraffin slices of three *P. mume* variety one-year-old branches under cryogenic treatment. A-G indicate temperatures of 4, -5, -10, -15, -20, -25, and -30 °C, respectively. The three varieties were sorted as: 1, DF; 2, XR; and 3, BY. Ep, epidermal cell; Co, cortex; Ph, phloem; Pf, phloem fiber; Xy, xylem; Pi, pith. The red arrows point to images observed in paraffin sections of the third node of the branch from top to bottom in the red box, respectively.

Unlike stems, buds protect themselves from cold temperatures by keeping water in their cells for undercooling to avoid freezing [46]. Therefore, the morphological data showed that there was no recovery ability of the flower buds and leaf buds after freezing injury (Figure 5A). We calculated the survival rates of buds after different temperature treatments (Figure 5B,C). The changes in the trends of leaf buds and flower buds were

consistent among the three varieties. The survival rate of DF was the highest, and that of XR was the second highest, while the survival rate of BY was the lowest. Different tissue comparisons revealed that leaf buds had a higher rate of viability than flower buds. The leaf buds were still viable at $-20\text{ }^{\circ}\text{C}$, but the flower buds were fragile. The results suggest that the leaf buds were more cold-tolerant than the flower buds.

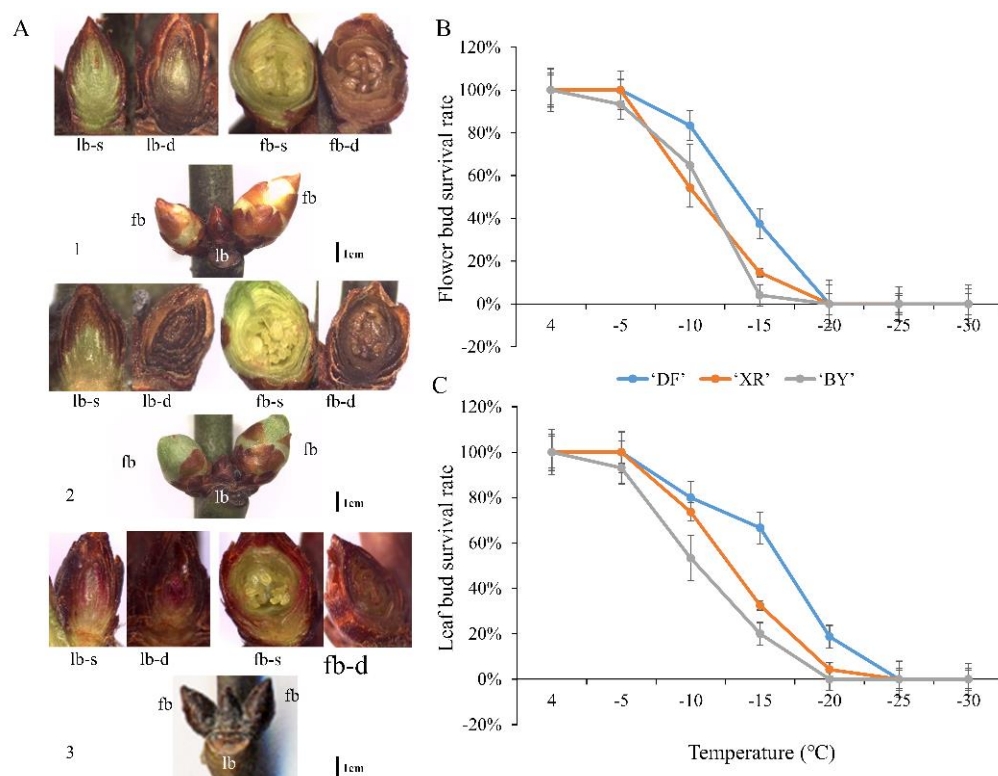


Figure 5. Anatomical states of survival or frozen death of leaf buds and flower buds, and survival rates of three *P. mume* varieties. Morphological and anatomical images of flower buds (fb) and leaf buds (lb): (A), 1–3 are BY, XR, and DF, respectively. lb-s, leaf bud survival; lb-d, leaf bud death; fb-s, flower bud survival; fb-d, flower bud death. Flower bud (B) and leaf bud (C) survival rate of three *P. mume* varieties.

3.3. Antioxidant Enzymes SOD and POD Induce Cold Acclimation Ability of XR

Antioxidant enzymes have the function of converting peroxide formation in plants into less toxic or harmless substances, so the SOD and POD antioxidant enzyme activities of mei were determined. In stage 3 in Figure 6, the three varieties experienced cold acclimation. The variation in the SOD content of BY was not obvious, and that of DF decreased more than three times; only the SOD content of XR gradually accumulated. The POD content of BY showed an overall decreasing process. It decreased by one-fold after cold acclimation, and there was no significant change when freezing. FH remained around $2\text{ U}\cdot\text{g}^{-1}\cdot\text{min}^{-1}$, with a small decrease after cold acclimation. The results for XR gradually increased during cold acclimation and decreased when freezing. A comparative analysis of the three varieties showed that the SOD and POD enzyme activities of XR were elevated after cold acclimation, suggesting it may enhance its cold tolerance by increasing antioxidant enzyme activity (Figure 6B).

The transcriptome data were used to mine XR for DEGs (differential expression genes). During cold acclimation, SOD- and POD-enzyme-related differential genes were mapped on a heat map (Figure 6A). The DEGs were classified into two classes based on a cluster analysis. The FPKM values for class II of the *PmSOD* genes were all higher than those of class I. The expression of *PmSOD3* was significantly higher than the other genes in class II, with the highest value exceeding 1000 FPKM. These results made *PmSOD3* a key gene

for the enhancement of SOD enzyme activity. The expression of POD-related genes in class II was higher than that in class I. All the class I genes were upregulated during the cold response and acclimation periods (stages 2 and 3, respectively, in Figure 6A). Among them, *PmPOD2* had the highest FPKM value, suggesting it might be greatly involved in POD enzyme synthesis. *PmPOD19* and 22 were not clustered in the same class, but their expression trends in the cold acclimation period of XR were similar, and their expression levels showed two-fold and nine-fold increases from the control, respectively. These results were consistent with the trends in POD enzyme activity. However, their expressions were still elevated in the freezing period, while enzyme activity was not. This phenomenon could be produced by the inhibition of gene regulation by ice crystals in the cells and tissues.

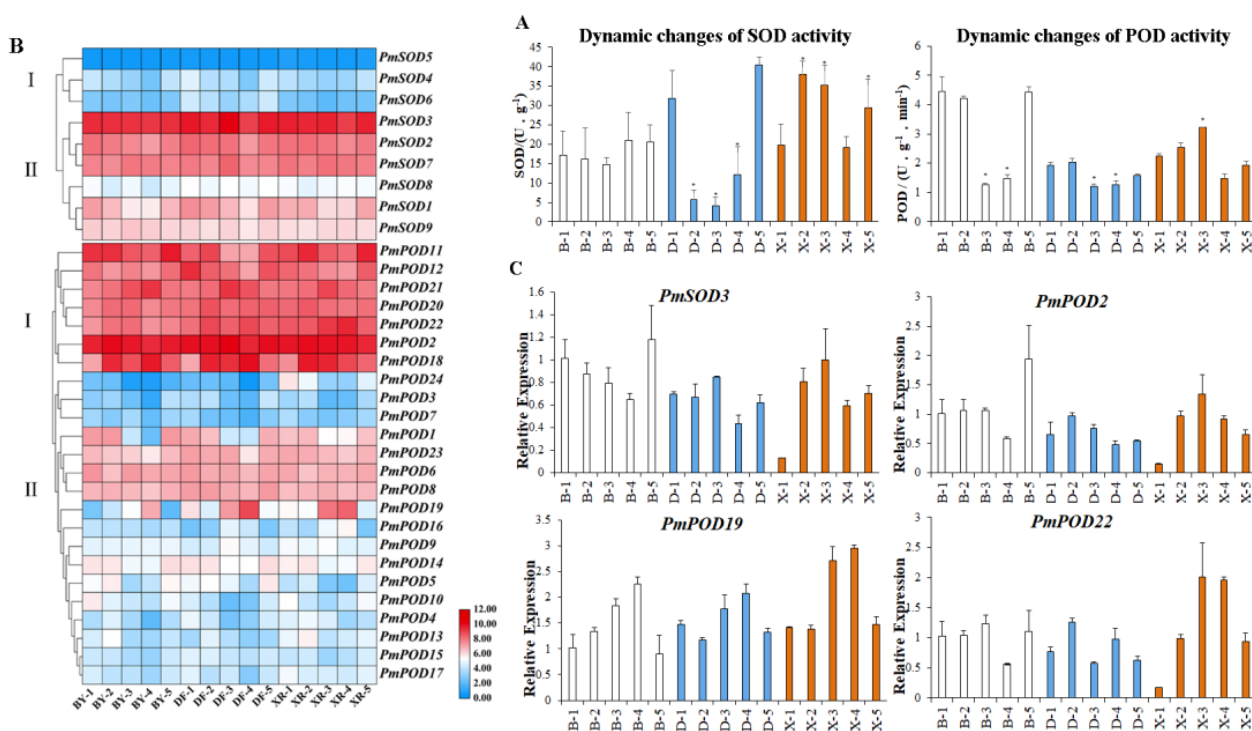


Figure 6. SOD and POD enzyme activity changes and encoding gene expression patterns of three *P. mume* varieties under cold stress: (A) measurement of SOD and POD enzyme activities ($p < 0.05$, marked by *); Heatmap (B); and relative expressions (C) of genes encoding SOD and POD enzymes in *P. mume* in response to cold. B, D, and X in axis X refer, respectively, to BY, DF, and XR, and 1–5 refer to different stages of cold treatment: 1 is control, at which the ambient temperature was 25 °C; 2 is 4 °C treatment for 8 h; 3 is 4 °C treatment for 5 d; 4 is temperature drop to −5 °C; and 5 is temperature increase to 15 °C after cold treatment. A rate of 1 °C per hour was maintained throughout the rise and fall stabilization process.

To further comprehensively investigate *PmSOD* and *PmPOD* functions in low temperatures, the four genes were detected with qRT-PCR experiments in which the stems of *P. mume* experienced chilling treatment (4 °C for 8 h and 5 d) and freezing treatment (−5 °C for 1 h). The expressions were distinct in the three varieties of *P. mume* (Figure 6C). All four genes were significantly elevated in XR during cold acclimation, which was consistent with the trends in changes for SOD and POD, positively regulating enzyme activity.

4. Discussion

The evaluation of cold tolerance has an important role in the selection and breeding of plant varieties. Previous researchers have assessed the degrees of low-temperature stress in plants during overwintering through field observations and indoor programmed cooling experiments [56], including the tolerance of *Carex* [57], *Prunus persica* [58], *Prunus*

mume [1,7], *Berberis thunbergii* [58], and *Lily* [59]. The cold tolerance abilities of 38 varieties representing the *P. mume* system, classes and types were already compared by Zhang in 1985 [6]. Based on the former, we added a cold tolerance analysis of the new varieties in the field. The cold tolerance of the apricot mei DF was higher than that of BY, which is consistent with Zhang's tolerance results [6,26]. Additionally, the tolerance of the new variety XR was in the middle of the parental results. An infrared dynamic observation of icing and freezing revealed that XR was the same as DF for freezing-point temperature, with relatively low results in the stem but higher in the bud. An even better finding was that the cold acclimation ability of XR was particularly impressive.

Monitoring the freezing of water in different tissues of plants at low temperatures can help explain the mechanisms of freezing tolerance in different varieties. There were significant differences in the freezing-point temperatures of water in the stems and buds of different varieties of mei under low-temperature treatments. The freezing-point temperatures of the three varieties were measured using infrared technology and tree moisture detection, which is a newly developed monitoring technique. The freezing-point temperatures of one-year-old stems of the apricot mei varieties XR and DF ranged from $-4\text{ }^{\circ}\text{C}$ to $-6\text{ }^{\circ}\text{C}$, which were lower than that of true *mume* BY (between $-3\text{ }^{\circ}\text{C}$ and $-4\text{ }^{\circ}\text{C}$). As the temperature can vary up to $15\text{ }^{\circ}\text{C}$ over a day in Beijing [60], the apricot mei DF could resist cold temperatures by avoiding ice formation in the branches, but the true *mume* BY was prone to irreversible mechanical damage from repeated freezing and thawing. The bud freezing-point temperature of BY ranged from $-7\text{ }^{\circ}\text{C}$ to $-8\text{ }^{\circ}\text{C}$, and was significantly lower than the two apricot mei varieties (between $-6\text{ }^{\circ}\text{C}$ and $-7\text{ }^{\circ}\text{C}$). The reason for the difference could be that the mechanism of water subcooling in the buds of the true *mume* was different from that of the apricot mei varieties.

Oxidative stress and cellular antioxidant capacity are assumed to be essential factors in the aging process of plants [19]. Our study confirmed that improving antioxidant capacity during low-temperature acclimation could stimulate a strong cold tolerance in XR, which may help its open-field cultivation in the north. In addition, most apricot mei varieties are missing the characteristic aroma of mei, while XR is one of the few apricot mei varieties that has the genotype of apricot mei with the characteristic aroma of true *mume* [10,61]. It has great potential for development and distribution in the market.

5. Conclusions

Based on the results of this study, we presented a preliminary schematic diagram of changes in the response of XR stem cells at low temperatures in a cellular anthropomorphic manner (Figure 7). The stem cells were in a normal state of life in the temperature range of $15\text{--}25\text{ }^{\circ}\text{C}$. In the process of gradual cooling from $15\text{ }^{\circ}\text{C}$ to $0\text{ }^{\circ}\text{C}$, the cells felt cold and increased the expressions of SOD- and POD-related genes through cell membrane phase change, calcium ions, and other signal regulation. This change further regulated the SOD and POD enzyme activities, as well as other antioxidant secondary metabolites. The increase in enzyme activity enhanced the antioxidant capacity of XR to avoid cell decay. Signals such as cell membrane phase change and calcium ions also regulated the accumulation of osmoregulatory substances to keep intracellular water in a liquid state at temperatures below $0\text{ }^{\circ}\text{C}$. Ambient temperatures below the freezing-point temperature ($-6\text{ }^{\circ}\text{C}$) caused the cells to gradually freeze, but cells experienced rupture and death once the temperature increased again. This process of change at low temperatures is only a summary and speculation based on the results of this study, and the specific regulatory mechanism remains to be further investigated.

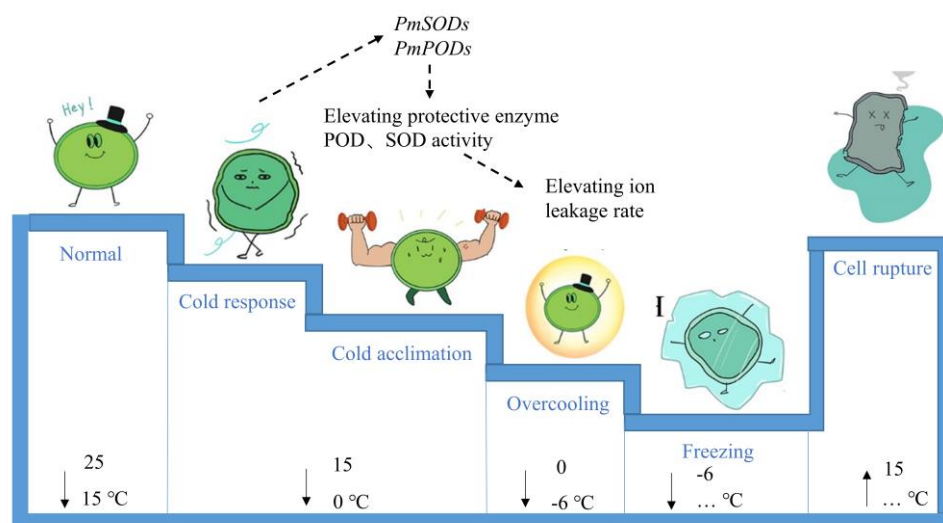


Figure 7. Different stages of low-temperature response of apricot mei XR.

Supplementary Materials: The following supporting information can be downloaded at: <https://www.mdpi.com/article/10.3390/f13122163/s1>, Figure S1: Adult trees and annual grafted seedlings of three *P. mume* varieties. Mature tree (A–C) and grafted seedlings (D): *P. mume* ‘Beijing Yudie’ (A,D-1), *P. mume* ‘Xiang Ruibai’ (B,D-2), *P. mume* ‘Dan Fenghou’ (C,D-3). Materials for moisture monitoring during the whole winter stage: *P. mume* ‘Beijing Yudie’ (E), *P. mume* ‘Dan Fenghou’ (F). Figure S2: Calculated standard curve for moisture monitoring of *P. mume* ‘Beijing Yudie’ (a), *P. mume* ‘Dan Fenghou’ (b). Figure S3: Dynamic video of three *P. mume* varieties freezing exothermic process. Figure S4: Dynamic video of *P. mume* stems freezing exothermic process. Figure S5: Dynamic video of *P. mume* flowerbuds freezing exothermic process. Table S1: Primer sequences for RT-qPCR in *P. mume*.

Author Contributions: Q.Z. supported resources. A.D. (Anqi Ding) and F.B. conceived and designed research. A.D. (Anqi Ding) conducted experiments, analyzed data, and wrote the original draft. F.B. reviewed and edited the manuscript. A.D. (Aiqin Ding) supported resources. All authors have read and agreed to the published version of the manuscript.

Funding: This research was supported by the National Key R&D Program of China (2019YFD1001500) and Special Fund for Beijing Common Construction Project.

Acknowledgments: We thank Zhao Yandong and his team Gao Chao, Tian Hao, Gu Jiahua, Li Bo and Sun Zhe from the School of Engineering, Beijing Forestry University for supporting the research on Infrared Video and Stem Water Content in this paper. And Thanks to Liu Yichi from Rangsit University in Thailand for her art guidance in Figure 7. Thanks to our team for supporting this research. Finally we would like to highlight our thanks to the editors and reviewers of *Forests* for their guidance and acceptance of this paper.

Conflicts of Interest: The authors have declared that no competing interests exist.

References

- Chen, J. Sixty years of *Prunus mume* research. *J. Beijing For. Coll.* **2002**, *Z1*, 224–229.
- Chen, J. *Prunus Mume Species Atlas in China*. China Forestry Publishing House: Beijing, China, 2010; pp. 10–11. ISBN 978-7-5038-5539-9.
- Chen, J. Study on *Prunus mume* in China—experiment on introduction and domestication of *Prunus mume*. *Acta Hortic. Sin.* **1963**, *2*, 395–410.
- Chen, J.; Zhang, Q. Study on cold resistance breeding and regional test of *Prunus mume*. *J. Beijing For. Coll.* **1995**, *17*, 42–45.
- Chen, J.; Chen, R. On the classification system of *Prunus mume* cultivars. *Acta Hortic.* **2007**, *34*, 1055–1058. [[CrossRef](#)]
- Zhang, Q. Comparative analysis of cold resistance of *Prunus mume*. *J. Beijing For. Coll.* **1985**, *02*, 47–56.
- Li, Q. Preliminary report on regional test of cold-resistant *Prunus mume* varieties in Urumqi. *J. Beijing For. Coll.* **2012**, *S1*, 50–55.
- Duan, M.; Li, W.; Gao, X.; Sun, Y.; Li, Q. Study on cold resistance of three *Prunus mume* varieties. *Res. Prog. Ornament. Hortic. China* **2015**, *S685.17*, 504–508.

9. Jiang, L.; Chen, J. A brief introduction to “transferring *Prunus mume* from south to north”—performance and prospect. *China Landsc. Archit.* **2011**, *27*, 1.
10. Chen, R.; Zhang, Q.; Chen, J. A new aromatic cold-resistant *Prunus mume* variety—‘Xiangruibai’. In Proceedings of the National Symposium on Flower Research and Production Technology Development Facing the New Century, Nanjing, China, 24–26 August 2005; S334, pp. 30–34.
11. Hughes, M.A.; Pearce, R.S. Low temperature treatment of barley plants causes altered gene expression in shoot meristems. *J. Exp. Bot.* **1988**, *39*, 1461–1467. [[CrossRef](#)]
12. McCully, M.E.; Canny, M.J.; Huang, C.X. The management of extracellular ice by petioles of frost-resistant herbaceous plants. *Ann. Bot.* **2004**, *94*, 665–674. [[CrossRef](#)]
13. Pearce, R.S. Extracellular ice and cell shape in frost-stressed cereal leaves: A low-temperature scanning-electron-microscopy study. *Planta* **1988**, *175*, 313–324. [[CrossRef](#)]
14. Kodama, H.; Horiguchi, G.; Nishiuchi, T.; Nishimura, M.; Iba, K. Fatty acid desaturation during chilling acclimation is one of the factors involved in conferring low-temperature tolerance to young *Tobacco* leaves. *Plant Physiol.* **1995**, *107*, 1177–1185. [[CrossRef](#)]
15. Chinnusamy, V.; Zhu, J.; Zhou, T.; Zhu, J.K. Small RNAs: Big role in abiotic stress tolerance of plants. In *Advances in Molecular Breeding Toward Drought and Salt Tolerant Crops*; Springer: Dordrecht, The Netherlands, 2007.
16. Shi, Y.; Ding, Y.; Yang, S. Cold signal transduction and its interplay with phytohormones during cold acclimation. *Plant Cell Physiol.* **2015**, *56*, 7–15. [[CrossRef](#)]
17. Thomashow, M.F.; Stockinger, E.J.; Jaglootosen, K.; Zarka, D.; Gilmour, S.J. Method for regulating cold and dehydration regulatory genes in a plant. U.S. Patent US5891859A, 06 April 1999.
18. Xueming, G.; Jianzhen, L.; Yongjun, L.; Xiao, X.; Rongfu, G. Overview of cold resistance of woody plants. *Subtrop. Plant Sci.* **2014**, *43*, 329–338.
19. Pearce, R.S.; Ashworth, E.N. Cell shape and localisation of ice in leaves of overwintering wheat during frost stress in the field. *Planta* **1992**, *188*, 324–331. [[CrossRef](#)]
20. Yao, S. Depth cold of fruit trees. *Deciduous Fruit Tree* **1991**, *01*, 034.
21. Fujikawa, S.; Kuroda, K. Cryo-scanning electron microscopic study on freezing behavior of xylem ray parenchyma cells in hardwood species. *Micron* **2000**, *31*, 669–686. [[CrossRef](#)]
22. Burke, M.J.; Stushnoff, C. Frost hardiness: A discussion of possible molecular causes of injury with particular reference to deep supercooling of water. In *Stress Physiology of Crop Plants*; John Wiley & Sons: New York, NY, USA, 1979; pp. 199–226.
23. Lyons, J.M.; Raison, J.K.; Kumamoto, J. Polarographic determination of phase changes in mitochondrial membranes in response to temperature. In *Methods in Enzymology*; Academic Press: Cambridge, MA, USA, 1974; Volume 32, pp. 258–262.
24. Améglio, T.; Cochard, H.; Ewers, F.W. Stem diameter variations and cold hardiness in walnut trees. *J. Exp. Bot.* **2001**, *52*, 2135–2142. [[CrossRef](#)]
25. Cottee, N.S.; Tan, D.K.Y.; Bange, M.P.; Cheetham, J.A. Simple electrolyte leakage protocols to detect cold tolerance in *cotton* genotypes. In Proceedings of the 4th World Cotton Research Conference, Lubbock, TX, USA, 10–14 September 2007; Volume 9, pp. 31–35.
26. Zhang, Q. *Prunus mume* hybridization and cold tolerance breeding—Study on frost resistance of hybrids and their parents. *J. Beijing For. Coll.* **1988**, *04*, 53–59.
27. Steponkus, P.L. Role of the plasma membrane in freezing injury and cold acclimation. *Annu. Rev. Plant Physiol.* **1984**, *35*, 543–584. [[CrossRef](#)]
28. Fei, W. Cold resistance determination of apricot flower dates with electrolyte leakage and logistic equation. *Acta Univ. Agric. Bpreali-Occident.* **1997**, *25*, 59–63.
29. Atiyeh, O.; Ali, T.; Ahmad, N.; Mahmoud, S. Effects of drought stress on cold hardiness of non-acclimated *viola* (*Viola × wittrockiana* ‘Iona Gold with Blotch’) in controlled conditions. *Sci. Hortic-Amst.* **2018**, *238*, 98–106.
30. Ahmad, S.K.; Muhammad, J.A.; Zora, S. Increased ethylene biosynthesis elevates incidence of chilling injury in cold-stored ‘Amber Jewel’ Japanese plum (*Prunus salicina* Lindl.) during fruit ripening. *Int. J. Food Sci. Technol.* **2011**, *46*, 642–650.
31. Peng, L.; Wang, M.; Liang, W. Indexing cold tolerance/resistance of Hazelnut. *HortScience A Publ. Am. Soc. Hortic. Sci.* **1996**, *31*, 645d–645. [[CrossRef](#)]
32. Su, L.; Dai, Z.; Li, S.; Xin, H. A novel system for evaluating drought–cold tolerance of *grapevines* using chlorophyll fluorescence. *BMC Plant Biol.* **2015**, *15*, 1–12. [[CrossRef](#)] [[PubMed](#)]
33. Karami, H.; Rezaei, M.; Sarkhosh, A.; Rahemi, M.; Jafari, M.J.G.P. Cold Hardiness Assessment in Seven Commercial Fig Cultivars (*Ficus carica* L.). *Gesunde Pflanz.* **2018**, *70*, 195–203. [[CrossRef](#)]
34. Stushnoff, C. Breeding and selection methods for cold hardiness in deciduous fruit crops. *Hortscience A Publ. Am. Soc. Hortic. Sci.* **1972**, *7*, 10–13.
35. Pauliina, P.; Deborah, B. Current state of cold hardiness research on fruit crops. *Can. J. Plant Sci.* **1997**, *77*, 399–420.
36. En, A.; Me, W. Response of fruit tree tissues to freezing temperatures. *Hortscience A Publ. Am. Soc. Hortic. Sci.* **1991**, *26*, 2135–2142.
37. Yang, S.; Tyree, M.T. A theoretical model of hydraulic conductivity from embolism with comparison to experimental data on *Acer saccharum*. *Plant Cell Environ.* **1992**, *15*, 633–643. [[CrossRef](#)]
38. Sperry, J.S.; Sullivan, J.E.M. Xylem embolism in response to freeze-thaw cycles and water stress in ring-porous, diffuse-porous, and conifer species. *Plant Physiol.* **1992**, *100*, 605–613. [[CrossRef](#)]

39. Hacke, U.G.; Sperry, J.S. Functional and ecological xylem anatomy. *Perspectives in Plant Ecology Evolution Systematics*. **2001**, *4*, 97–115. [[CrossRef](#)]
40. Sundblad, L.G.; Andersson, M.; Geladi, P.; Salomonson, A.; Sjoström, M. Fast, nondestructive measurement of frost hardiness in conifer seedlings by VIS+NIR spectroscopy. *Tree Physiol.* **2001**, *21*, 751–757. [[CrossRef](#)]
41. Gamble, G.R. Non-Invasive determination of freezing effects in blueberry fruit tissue by magnetic resonance imaging. *J. Food Sci.* **1994**, *59*, 571–573. [[CrossRef](#)]
42. Liu, D.; Faust, M.; Millard, M.M.; Line, M.J.; Stutte, G.W. States of water in summer-dormant apple buds determined by proton magnetic resonance imaging. *J. Am. Soc. Hortic. Sci. Am. Soc. Hortic. Sci.* **1993**, *118*, 632–637. [[CrossRef](#)]
43. Wronski, E.B.; Holmes, J.W.; Turner, N.C. Phase and amplitude relations between transpiration, water potential and stem shrinkage. *Plant Cell Environ.* **1985**, *8*, 613–622. [[CrossRef](#)]
44. Wisniewski, M.; Glenn, D.M.; Gusta, L.V.; Fuller, M.; Griffith, M. Using infrared thermography to study ice nucleation and propagation in plants. *Acta Hortic.* **2003**, *618*, 485–492. [[CrossRef](#)]
45. Wisniewski, M.; Gusta, L.; Neuner, G. Adaptive mechanisms of freeze avoidance in plants: A brief update. *Environ. Exp. Bot.* **2014**, *99*, 133–140. [[CrossRef](#)]
46. Kuprian, E.; Briceo, V.F.; Wagner, J.; Neuner, G. Ice barriers promote supercooling and prevent frost injury in reproductive buds, flowers and fruits of alpine dwarf shrubs throughout the summer. *Environ. Exp. Bot.* **2014**, *106*, 4–12. [[CrossRef](#)]
47. Gao, C.; Zhao, Y.; Zhao, Y. A novel sensor for noninvasive detection of in situ stem water content based on standing wave ratio. *J. Sens.* **2019**, 1–10. [[CrossRef](#)]
48. Sun, Y.; Zhou, H.; Shan, G.; Grantz, D.A.; Schulze Lammers, P.; Xue, X.; Damerow, L.; Burkhardt, J. Diurnal and seasonal transitions of water and ice content in apple stems: Field tracking the radial location of the freezing- and thawing-fronts using a noninvasive smart sensor. *Agric. For. Meteorol.* **2019**, *274*, 75–84. [[CrossRef](#)]
49. Zhao, Y.; Gao, C.; Zhang, X.; Xu, Q. Non-destructive measurement of plant stem water content based on standing wave ratio. *Trans. Chin. Soc. Agric. Mach.* **2016**, *47*, 310–316.
50. Zhou, H.; Sun, Y.; Shan, G.; Grantz, D.A.; Cheng, Q.; Schulze Lammers, P.; Damerow, L.; Wen, B.; Xue, X.; Chen, B. In situ measurement of stem water content and diurnal storage of an apricot tree with a high frequency inner fringing dielectric sensor. *Agric. For. Meteorol.* **2018**, *250*, 35–46. [[CrossRef](#)]
51. Tian, H.; Gao, C.; Zhao, Y.; Zheng, Y.; Zhao, Y. Design and analysis of freeze-thaw detection sensor for standing forest stock based on latent heat. *Trans. Chin. Soc. Agric. Mach.* **2020**, *51*, 223–231.
52. Lim, C.C.; Arora, R.; Townsend, E.C. Comparing gompertz and richards functions to estimate freezing injury in *Rhododendron* using electrolyte leakage. *J. Am. Soc. Hortic. Sci. Am. Soc. Hortic. Sci.* **1998**, *123*, 246–252. [[CrossRef](#)]
53. Ying, Y.; Rao, X.; Huang, Y. Methodology for images grabbing of massive numbers of moving fruits. *Zhejiang Univ.* **2004**, *02*, 32–37.
54. Li, H.; Sun, Q.; Zhao, S.; Zhang, W. *Assay of Malondialdehyde in Plants Experiment Principle and Technology of Plant Physiology and Biochemistry*; Higher Education Press: Beijing, China, 2000; pp. 260–261.
55. Ding, A.; Bao, F.; Zhang, T.; Yang, W.; Wang, J.; Cheng, T.; Zhang, Q. Screening of optimal reference genes for qRT-PCR and preliminary exploration of cold resistance mechanisms in *Prunus mume* and *Prunus sibirica* varieties. *Mol. Biol. Rep.* **2020**, *47*, 6635–6647. [[CrossRef](#)]
56. Soderholm, P.K.; Gaskins, M.H. Evaluation of cold resistance in the genus *Coffea*. *Biology* **1960**, *4*, 8–15.
57. Ye, Y.R.; Wang, W.L.; Zheng, C.S.; Fu, D.J.; Liu, H.W. Evaluation of cold resistance of four wild *Carex* species. *J. Appl. Ecol.* **2017**, *28*, 89–95.
58. Wang, Q.; Xiao-Nan, Y.U. Physiological response to low temperature stress and evaluation of cold resistance of three color-leafed trees. *J. Beijing For. Univ.* **2013**, *35*, 104–109.
59. Liu, Y.; Zhu, Y.; Kang, X.; Zhang, J. Evaluation of cold resistance of different types of *Magnolia grandiflora*. *Sci. Silvae Sin.* **2013**, *49*, 178–183.
60. Zhao, D.; Wu, J. Comparisons of urban-related warming in Beijing using different methods to calculate the daily mean temperature. *Ence China Earth Ence* **2019**, *62*, 89–98. [[CrossRef](#)]
61. Bao, F.; Zhang, T.; Ding, A.; Ding, A.; Yang, W.; Wang, J.; Cheng, T.; Zhang, Q. Metabolic, Enzymatic Activity, and Transcriptomic Analysis Reveals the Mechanism Underlying the Lack of Characteristic Floral Scent in Apricot Mei Varieties. *Front. Plant Sci.* **2020**, *11*, 574982. [[CrossRef](#)]